Metallic nanosphere-assisted coupling ultrafast surface plasmon polaritons background-free tip nanofocusing

CHAO MENG,[1] WEIJIAN LI,[1] ZHONGLIN XIE,[1] LU ZHANG,[1] LEI XU,[2,4] FENG GAO,[3] WENDING ZHANG,[1,*] TING MEI,[1] AND JIANLIN ZHAO[1]

[1]*Key Laboratory of Light Field Manipulation and Information Acquisition, Ministry of Industry and Information Technology, and Shaanxi Key Laboratory of Optical Information Technology, School of Physical Science and Technology, Northwestern Polytechnical University, Xi'an 710129, China.*

[2]*Advanced Optics & Photonics Laboratory, Department of Engineering, School of Science & Technology, Nottingham Trent University, Nottingham NG11 8NS, United Kingdom*

[3]*MOE Key Laboratory of Weak-Light Nonlinear Photonics, TEDA Applied Physics Institute and School of Physics, Nankai University, Tianjin 300457, China*

[4]*lei.xu@ntu.ac.uk*

**Corresponding author: zhangwd@nwpu.edu.cn*

Received XX Month XXXX; revised XX Month, XXXX; accepted XX Month XXXX; posted XX Month XXXX (Doc. ID XXXXX); published XX Month XXXX

Plasmonic tip nanofocusing has gained much attention owing to its wide application in the field of nanospectroscopy. Here, we present the gold nanosphere (AuNS)-assisted coupling ultrafast surface plasmon polaritons (SPP) background-free tip nanofocusing. The plasmonic tip was prepared by attaching an AuNS on the shaft of an Au conical tip fabricated by electrochemical etching. The AuNS was adopted as an antenna to couple the far-field excitation light to the propagating SPP along the shaft to the tip apex for achieving power compression. Importantly, we experimentally and theoretically demonstrate that such a plasmonic tip can realize background-free ultrafast SPP tip nanofocusing with radially-polarized feature in a wide spectral range based on the localized surface plasmon polaritons resonance effect supported by AuNS. Furthermore, the intensity of the tip nanofocusing light field has a strong polarization-dependent under linearly polarized light excitation, providing a powerful platform for spatiotemporal light control on the nanoscale. Our technique realizes remote excitation of background-free tip nanofocusing with structured light feature, it holds promising potential for tip-enhanced nanospectroscopies and nonlinear nanophotonics, etc.

http://dx.doi.org/10.1364/OL.99.099999

Tip-enhanced nanospectroscopy (TENS) is a rapidly developing research field, and has developed many types of super-resolution imaging methods, such as tip-enhanced Raman spectroscopy [1-3], tip-enhanced photoluminescence nanoimaging [4], tip-enhanced hot-electron nanoscopy [5], tip-enhanced four-wave mixing nanoimaging [6-8], tip-enhanced coherent anti-stokes Raman microscopy [9], etc. Based on the ultrasensitive tip-enhanced nanospectral platforms, the structure information of the analytes can be obtained with high spatial resolution, even reaches the single-molecule level [2,3].

TENS is the combination of a scanning probe microscope and a plasmonic tip, and the production reproducibility of plasmonic tip with excellent nanofocusing characteristic determine the performance of TENS [10]. A sharp metallic tip is commonly used in TENS, in which the tip nanofocusing light field with radial polarization is generated by directly irradiating the tip apex via a focused far-field excitation light. Because the size of the focused spot (~0.5 μm) is much larger than the curvature radius of the tip apex (~10 nm), the uncoupled light focused on the surface of the analytes can also simultaneously excite the background noise [11], which in turn reduces the sensitivity and spatial resolution of TENS system.

To achieve the background-free tip nanofocusing, Ropers *et al.* proposed the grating-assisted coupling plasmonic tip in 2007 [12], where the grating was etched on the shaft away from the tip apex of ~10 μm. The grating coupled the far-field excitation light as the surface plasmon polaritons (SPP), which then propagated along the shaft to the tip apex to achieve power compression. Due to the effective separation of the far-field excitation light and the tip apex, the background-free tip nanofocusing can be achieved. The grating-assisted coupling tip has been explored in the fields of hot-electron nanoscopy [5], ultrafast coherent nonlinear nanoscopy [7], selective CARS microscopy [9], white nanolight source-based nanoimaging [13], etc. Nevertheless, processing the grating on the tip shaft requires the focused ion beam etching, which is a relatively complicated and high-cost preparation method.

In 2018, another type of remote-excitation plasmonic tip was proposed [14]. An Ag nanocube (AgNC) was attached on the shaft of an Ag nanowire (AgNW) with the ultrasharp tip curvature radius of ~10 nm. The AgNC was used to couple the far-field excitation

light to propagating SPP along the shaft of the AgNW to the tip apex to achieve background-free nanofocusing. The AgNW with ultrasharp tip was prepared in batches by chemical synthesis [15]. Thus, the AgNW tips had uniform curvature radius to ensure that the tip nanofocusing had relatively consistent electric-field intensity and mode-field volume, simultaneously. Ag has a stronger plasmonic enhancement than Au in visible band, but has short-term stability due to easy oxidation. In addition, the AgNC-assisted coupling AgNW tip cannot be used directly, and must be fixed to the atomic force microscope (AFM) probe by micro-nano operation. The reproducibility of AFM-mounted AgNW probe is also a challenge. When the AFM probe, AgNW and AgNC are properly positioned in the three-dimensional space, the excitation light can irradiate the AgNC to achieve tip nanofocusing. Thus, it is challenge to precisely adjust the spatial position of the AFM probe, AgNW and AgNC through the micro-nano operation.

In this Letter, we present the AuNS-assisted coupling background-free plasmonic tip nanofocusing. The plasmonic tip was prepared by attaching an AuNS to the shaft of an Au conical tip fabricated by using electrochemical etching. The AuNS with diameter of 350 nm was used as an antenna to couple the far-field excitation light as propagating SPP along the shaft to the tip apex to achieve power compression. Theoretical and experimental results show that this plasmonic tip can realize background-free tip nanofocusing due to excellent localized surface plasmon resonance (LSPR) effect of AuNS in a wide spectral range, and the intensity of the tip nanofocusing light field has a strong polarization dependence on the linearly polarized excitation light. The traditional methods such as using high numerical aperture microscope objectives cannot obtain such highly-confined radially polarized light due to the diffraction limit.

Figure 1(a) is the sketch map of the AuNS-assisted coupling background-free tip nanofocusing. An AuNS was attached to the shaft of the Au conical tip. The distance between the AuNS and the tip apex is set as H=4 μm. The Au conical tip is parallel to the z-axis, and the wavevector K of the excitation light is in the x-z plane. The crossing angle between the wavevector K of the excitation light and the Au conical tip is defined as ϕ. θ is the crossing angle between the linear polarization direction of the excitation light and the z-axis. The tip curvature radius is R=20 nm. A femtosecond pulse (50 fs pulse duration) with central wavelength of 810 nm is used as the far-field excitation light, and the lasering spectrum is shown as the blue curve in Fig. 1(b). The diameter of AuNS is 350 nm, and its scattering spectrum was simulated using 3D finite-difference time domain (FDTD) method, as shown the red curve in Fig. 1(b). Note that the AuNS has excellent LSPR effect within the spectrum range of 550-900 nm [16], revealing that the femtosecond pulse can be effectively coupled to the ultrafast SPP to achieve tip nanofocusing.

The 3D FDTD method is further used to calculate the electric-field enhancement of the AuNS-assisted coupling plasmonic tip. The permittivity of Au is obtained from Johnson and Christy at λ=810 nm [17]. The perfectly matched layers are adopted as the absorption boundary to simulate the tip placed in an infinitely large free space. A uniform grid size of 1 nm was used in the volume 150 nm × 150 nm × 150 nm around the nanogap and the tip apex, while the other grid size was set as about λ/30. The focused linearly polarized femtosecond pulse was adopted as the excitation source. When the far-field excitation light is focused on the AuNS via a microscope objective (MO), it is converted to the SPP through the AuNS and then propagates along the tip shaft to form a nanofocusing light source at the tip apex. The electric-field enhancement factor is defined as $L=|E_{Tip}/E_{Excitation}|$, and the electric-field intensity enhancement factor (EF) is $EF=L^2$. Under condition of ϕ=0° and θ=0°, the normalized EF was calculated in case of MO with numerical aperture (NA) of NA=0.5, 0.7 and 0.9, as shown in Fig. 1(c). Note that the maximum EF can be obtained with NA=0.5. In addition, the EF can be further increased by reducing NA due to the transverse electric field component of the focused excitation light plays a vital role in EF (see Fig. S1 and Table. S1). Under condition of NA=0.5 and θ=0°, the normalized EF of the Au tip was calculated in case of ϕ=0°, 15°, 30°, 45°, and 60°, as shown in Fig. 1(d). The EF increases with the increase of ϕ, but ϕ=0 is adopted to facilitate subsequent experiments.

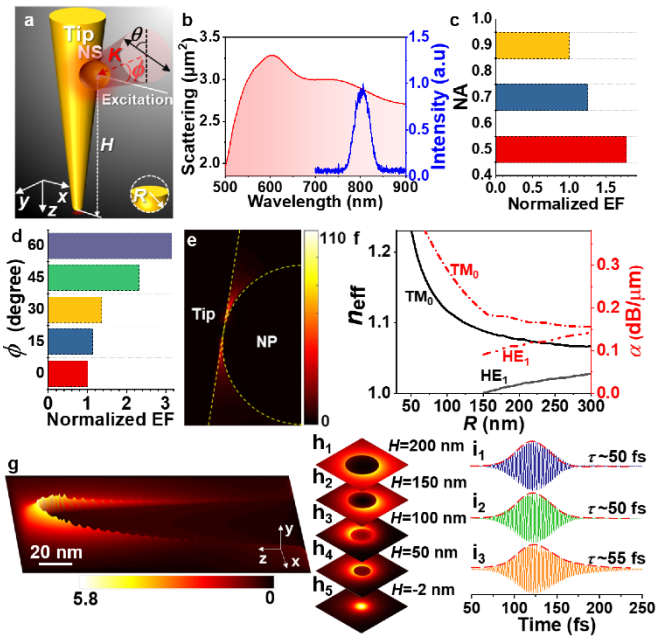

Fig. 1. (a) Sketch map of the AuNS-assisted coupling tip nanofocusing under a focused linearly polarized femtosecond pulse; (b) Scattering spectrum (red curve) of the AuNS with diameter of 350 nm, and the lasering spectrum (blue curve) of the femtosecond pulse. (c) Normalized EF with the relationship of NA; (d) Normalized EF with the relationship of ϕ; (e) Electric-field distribution at the junction between the tip shaft and the AuNS; (f) Effective indices n_{eff} and propagation loss α of the propagating SPP versus the tip radius; (g) Lateral electric-filed distribution of the propagating SPP in x-z plane; (h) Transverse modes intensity distributions of the propagating SPP in case of H=200 nm, 150 nm, 100 nm, 50 nm and -2 nm, respectively. Evolution process of the transverse mode intensity distributions along the tip (see Visualization 1); (i_1-i_3) Temporal evolution characteristics of the femtosecond pulses propagating along the shaft of the tip in case of H=4 μm, 2 μm, and -2 nm, respectively.

Figure 1(e) shows the electric-field distribution of the SPP with L=110 in the x-z plane when ϕ=θ=0°. The excited SPP propagates along the shaft of the Au tip. As the tip radius decreases, the high-order SPP mode is gradually cut off, but TM_0 mode with radial polarization is not cut off [18, 19], as shown in Fig. 1(f), which gives the effective indices n_{eff} and the propagation loss α as a function of

the tip radius R. Thus, only the TM_0 mode can propagate to the tip apex to achieve the tip nanofocusing. Figure 1(g) gives the lateral electric-field distribution of the tip in the x-z plane, and the transverse electric-field distributions of the propagating SPP under different H are shown in Figs. 1(h_1-h_5). Note that the high-order SPP mode is cut off, and only TM_0 mode propagates to the tip apex. When TM_0 mode approaches the tip apex, it no longer satisfies the adiabatic approximation condition due to the drastic change of the tip radius [20, 21], and further converts to the electromagnetic emission mode into free space. Figure 1(h_5) shows the transverse electric field distribution at the plane 2 nm (H=-2 nm) below the tip apex, its EF is smaller than that of the gap mode (L=110) due to the transmission loss of TM_0 mode. The temporal evolution characteristics of the femtosecond pulse propagating along the shaft of the tip is shown in Fig. 1(i). Figure 1(i_1) is the temporal waveform of the femtosecond pulse focused on the AuNS. Figures 1(i_2) and 1(i_3) are the temporal waveforms of the propagating SPP at the position of H=2 μm and -2 nm, respectively. The pulse duration was only stretched from 50 fs to 55 fs due to the small group delay dispersion of SPP propagating near the tip apex where the curvature radius changes sharply [22].

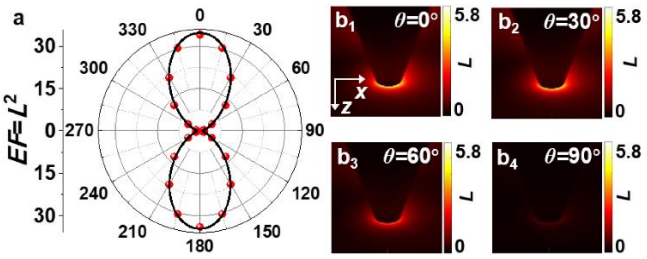

Fig. 2. (a) Relationship between EF and θ; (b_1-b_4) Electric-field distributions of SPP modes localized near the tip apex under condition of θ=0°, 30°, 60° and 90°, respectively.

Figure 2(a) gives the θ-dependent of the EF of the tip nanofocusing light field. The red dots are the calculated results, and the black curve is the theory fit with $EF(\theta)=EF_1\cos^2(\theta)+EF_0$, where EF_1 and EF_0 are the fit parameter. Figures 2(b_1-b_4) are the electric-field distribution of the SPP localized near the tip apex under condition of θ=0°, 30°, 60° and 90°, respectively. Note that the optimal electric-field enhancement of the tip nanofocusing can be obtained in the case of θ=0°.

An Au wire with diameter of 250 μm was used to fabricate the tip by electrochemical etching [23]. Then the tip was fixed laterally on a silicon wafer. 0.4 ml AuNS solution, with concertation of 9.1×10^{-4} mg/ml, was dropped on the tip apex and then let it stand for 24 hours. As shown in Fig. 3(a), the AuNS with diameter of 350 nm was modified to the shaft of the tip. The distance between the AuNS and the tip apex was 4 μm. The tip curvature radius was 20 nm, as shown the inset of Fig. 3(a). The structure parameters of the AuNS-assisted coupling tip were consistent with the theoretical calculation.

Figure 3(b) is the experimental setup to achieve the background-free tip nanofocusing. A linearly polarized femtosecond pulse (pulse duration: ~50 fs, central wavelength: 810 nm) was used as the excitation source. The AuNS-assisted coupling tip was fixed on a rotation mount (RM) to adjust the position of the AuNS to ensure that the excitation light can be vertically focused on the AuNS via a long working distance MO (100×, NA=0.5). The linear polarization direction θ of the excitation light, as shown the inset in Fig. 3(b), was adjusted via a half-wave plate (HWP). The tip emission light was collected by using another MO (20×, NA=0.4) in a 90° sagittal geometry, and detected with a charge coupled device (CCD). Inset in Fig. 3(c) is the lateral intensity distribution of the tip nanofocusing process in the x-z plane under condition of θ=0°. Note that the background-free tip nanofocusing has been achieved. Figures 3(c_1-c_4) are the intensity distribution of the tip nanofocusing light field measured in the case of θ=0°, 30°, 60° and 90°, respectively. Figure 3(d) is the horizontal intensity distributions through the centers of the lateral intensity distribution shown in Figs. 3(c_1-c_4). A polarizer (P) was inserted into the optical path to avoid oversaturation of the CCD. The square dots in Fig. 3(e) are the examination result of the θ-dependent of the tip nanofocusing, and the red curve is the theory fit with $I(\theta)=I_1\cos^2(\theta)+I_0$, where I_1 and I_0 are the fit parameter. In addition, the additional nanoparticles in the path of the propagating SPP should be eliminated to improve the tip nanofocusing efficiency (see Fig. S2), and the tip shaft should be as smooth as possible to reduce the propagation loss of SPP [10].

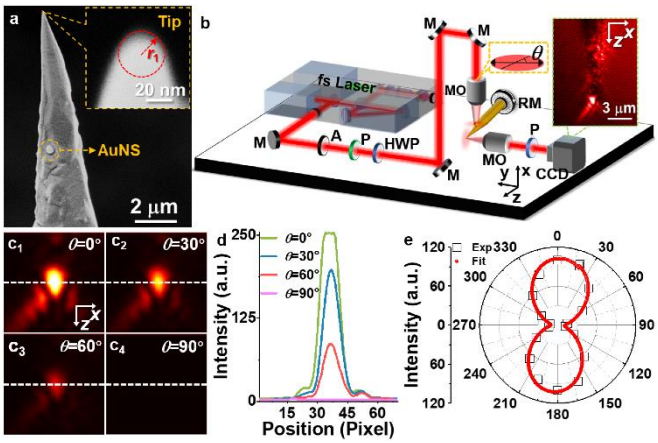

Fig. 3. (a) Scanning electric microscopy image of the AuNS-assisted coupling tip. Inset is the tip apex with curvature radius of ~20 nm. (b) Experimental setup of the AuNS-assisted coupling tip nanofocusing. M: mirror, A: attenuator, P: polarizer, HWP: half-wave plate, MO: micro-objective, RM: rotation mount, CCD: charge coupled device; (c_1-c_4) Intensity distribution of the tip nanofocusing light field in the case of θ=0°, 30°, 60° and 90°, respectively. (d) Horizontal intensity distributions through the centers of the lateral intensity distribution corresponding the patterns (c_1-c_4); (e) Relationship between θ and the intensity of the tip nanofocusing light field.

Figure 4(a) is the experimental setup for examining the transverse mode intensity and polarization distributions of the tip nanofocusing light field. Linearly polarized femtosecond pulse, with polarization direction paralleling to the axis of the tip, was vertically focused on the AuNS. A long working distance MO (NA=0.4) was adopted to axially collect the tip emission light, and imaged via a CCD. Figure 4(b) is the transverse mode intensity distribution of the tip emission light field with annular intensity patterns in absence of the polarizer. The non-uniform annular intensity distribution results from a small amount of remaining the AuNPs-coupled SPP [20, 24]. The mode intensity patterns at various polarizations of the polarizer are shown in Figs. 4(b_1-b_4). The examination result

revealing that the tip nanofocusing light field is TM_0 mode with radial polarization distribution. Figure 4(c) is the spectra of the excitation light (black curve) and the tip emission light field (red curve), revealing that the AuNS-assisted coupling tip has excellently broadband characteristics of the nanofocusing process. Figure 4(d) is the experimental result of θ-dependent of the tip emission spectrum. The square dots are the examination results obtained by subtracting the minimum value from the peak intensity of the emission spectrum, and the red curve is the theory fit result with $I(\theta)=I_1\cos^2(\theta)+I_0$, with I_1 and I_0 being of the fit parameter. Note that the experimental result is coincided with the theory fit. Furthermore, another seven AuNS-assisted tips were prepared using the same process. The examination results of the transverse mode intensity and polarization distribution (see Fig. S3) proved that this tip preparation method has excellent reproducibility.

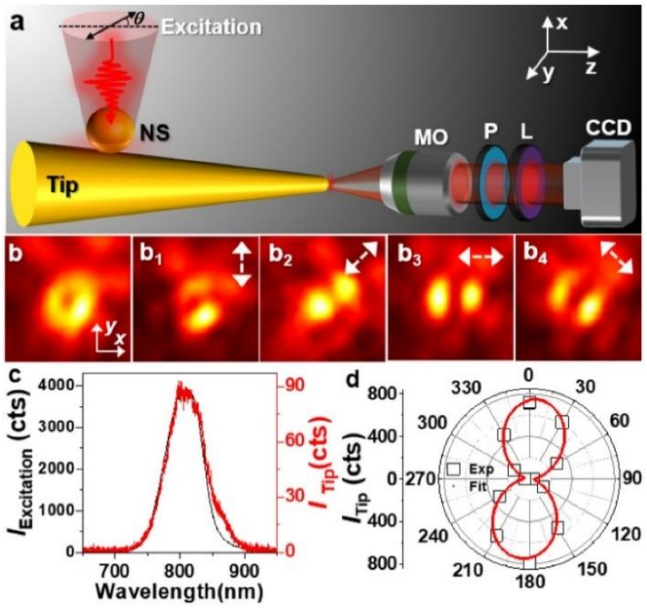

Fig. 4. (a) Experimental setup for examining the transverse mode intensity and polarization distributions of the tip nanofocusing light field. Transverse mode intensity distribution of TM_0 mode taken by CCD in absence of the polarizer (b) and in presence of the polarizer at different polarization orientations (b_1-b_4). The arrow represents the optical axis of the polarizer. (c) Spectra of the excitation light (black curve) and the tip emission spectrum (red curve); (d) Relationship between θ and the intensity of the tip emission spectrum.

In summary, we have presented the AuNS-assisted coupling background-free ultrafast SPP tip nanofocusing. The tip was prepared by attaching an AuNS on the shaft of an Au conical tip. The AuNS was used as an antenna to couple the far-filed excitation light as propagating SPP along the shaft to the tip apex to achieve power compression. Theoretical and experimental results show that this plasmonic tip can realize background-free tip nanofocusing with radial polarization in a wide spectral range, and the *EF* of the tip nanofocusing light field has a strong polarization-dependent for linearly polarized excitation light, providing a powerful platform for manipulating light and enhancing nanoscale light-matter interactions. Our proposed remote-excitation plasmonic tip may suggest promising potential in various nanophotonics applications, including nonlinear optics, tip-enhanced nanospectroscopy, etc.

Funding. National Natural Science Foundation of China (NSFC) (11974282, 91950207 and 11634010). National key R & D Program of China (2017YFA0303800). Fundamental Research Funds for the Central Universities (3102019JC008).

Disclosures. The authors declare no conflicts of interest.

Data availability. Data underlying the presented results are not publicly available at this time but may be obtained from the authors upon reasonable request.

Supplemental document. See Supplement 1 for supporting content.

REFERENCES

1. R. M. Stöckle, Y. D. Suh, V. Deckert, and R. Zenobi, Chem. Phys. Lett. **318**, 131 (2000).
2. R. Zhang, Y. Zhang, Z. C. Dong, S. Jiang, C. Zhang, L. G. Chen, L. Zhang, Y. Liao, J. Aizpurua, Y. Luo, J. L. Yang, and J. G. Hou, Nature **498**, 82 (2013)
3. J. Lee, K. T. Crampton, N. Tallarida, and V. A. Apkarian, Nature **568**, 78 (2019).
4. B. Yang, G. Chen, A. Ghafoor, Y. Zhang, Y. Zhang, Y. Zhang, Y. Luo, J. Yang, V. Sandoghdar, J. Aizpurua, Z. Dong, and J. G. Hou, Nat. Photon. **14**, 693 (2020).
5. A. Giugni, B. Torre, A. Toma, M. Francardi, M. Malerba, A. Alabastri, R. P. Zaccaria, M. I. Stockman, and E. D Fabrizio, Nat. Nanotech. **8**, 845 (2013).
6. T. Jiang, V. Kravtsov, M. Tokman, A. Belyanin, and M. B. Raschke, Nat. Nanotech. **14**, 838 (2019).
7. V. Kravtsov, S. AlMutairi, R. Ulbricht, A. R. Kutayiah, A. Belyanin, and M. B. Raschke, Phys. Rev. Lett. **120**, 203903. (2018).
8. V. Kravtsov, R. Ulbricht, J. M. Atkin, and M. B. Raschke, Nat. Nanotech. **11**, 459 (2016).
9. T. Ichimura, N. Hayazawa, M. Hashimoto, Y. Inouye, and S. Kawata, Phys. Rev. Lett. **92,** 220801 (2004).
10. Y. Fujita, P. Walke, S. D. Feyter, and H. Uji-i, Jpn. J. Appl. Phys. **55,** 08NB03 (2016).
11. S. Berweger, J. M. Atkin, R. L. Olmon, and M. B. Raschke, J. Phys. Chem. Lett. **1**, 3427 (2010).
12. C. Ropers, C. C. Neacsu, T. Elsaesser, M. Albrecht, M. B. Raschke, and C. Lienau, Nano. Lett. **7**, 2784 (2007).
13. T. Umakoshi, M. Tanaka, Y. Saito, and P. Verma, Sci. Adv. **6**, eaba4179 (2020).
14. X. Ma, Y. Zhu, N. Yu, S. Kim, Q. Liu, L. Apontti, D. Xu, R. Yan, and M. Liu, Nano. Lett. **19**, 100 (2019).
15. P. Walke, Y. Fujita, W. Peeters, S. Toyouchi, W. Frederickx, S. D. Feyter, and U. Hiroshi, Nanoscale **10**, 7556 (2018).
16. M. Kauranen, and A. V. Zayats, Nat. Photon. **6**, 737 (2012).
17. P. B. Johnson, and R. W. Christy, Phys. Rev. B **6**, 4370 (1972).
18. L. Novotny, and C. Hafner, Phys. Rev. E **50,** 4094 (1994).
19. M. Esmann, S. F. Becker, B. B. da Cunha, J. H. Brauer, R. Vogelgesang, P. Groß, and C. Lienau, Beilstein J. Nanotechnol. **4,** 603 (2013).
20. F. Lu, W. Zhang, L. Huang, S. Liang, D. Mao, F. Gao, T. Mei, and J. Zhao, Opto-Electron. Adv. **1**, 18001001 (2018).
21. M. I. Stockman, Phys. Rev. Lett. **93**, 137404 (2004).
22. S. Berweger, J. M. Atkin, R. L. Olmon, and M. B. Raschke, J. Phys. Chem. Lett. **3**, 945 (2012).
23. B. Ren, G. Picardi, and B. Pettinger, Rev. Sci. Instrum. **75**, 837 (2004).
24. S. Kim, N. Yu, X. Ma, Y. Zhu, Q. Liu, M. Liu, and R. Yan, Nat. Photon. **13**, 636 (2019).

Reference:

1. R. M. Stöckle, Y. D. Suh, V. Deckert, and R. Zenobi, Nanoscale chemical analysis by tip-enhanced Raman spectroscopy, Chem. Phys. Lett. 318(1–3), 131–136 (2000).
2. R. Zhang, Y. Zhang, Z. C. Dong, S. Jiang, C. Zhang, L. G. Chen, L. Zhang, Y. Liao, J. Aizpurua, Y. Luo, J. L. Yang, and J. G. Hou, Chemical mapping of a single molecule by plasmon-enhanced Raman scattering, Nature 498(7452), 82–86 (2013)
3. J. Lee, K. T. Crampton, N. Tallarida, and V. A. Apkarian, Visualizing vibrational normal modes of a single molecule with atomically confined light, Nature 568(7750), 78–82 (2019).
4. B. Yang, G. Chen, A. Ghafoor, Y. Zhang, Y. Zhang, Y. Zhang, Y. Luo, J. Yang, V. Sandoghdar, J. Aizpurua, Z. Dong, and J. G. Hou, Sub-nanometre resolution in single-molecule photoluminescence imaging, Nat. Photon. 14(11), 693–699 (2020).
5. A. Giugni, B. Torre, A. Toma, M. Francardi, M. Malerba, A. Alabastri, R. P. Zaccaria, M. I. Stockman, and E. D Fabrizio, Hot-electron nanoscopy using adiabatic compression of surface plasmons, Nat. Nanotech. 8(11), 845–852(2013).
6. T. Jiang, V. Kravtsov, M. Tokman, A. Belyanin, and M. B. Raschke, Ultrafast coherent nonlinear nanooptics and nanoimaging of graphene, Nat. Nanotech. 14(9), 838–843 (2019).
7. V. Kravtsov, S. AlMutairi, R. Ulbricht, A. R. Kutayiah, A. Belyanin, and M. B. Raschke, Enhanced Third-order optical nonlinearity driven by surface-plasmon field gradients, Phys. Rev. Lett. 120(20), 203903. (2018).
8. V. Kravtsov, R. Ulbricht, J. M. Atkin, and M. B. Raschke, Plasmonic nanofocused four-wave mixing for femtosecond near-field imaging, Nat. Nanotech. 11(5), 459–464 (2016).
9. T. Ichimura, N. Hayazawa, M. Hashimoto, Y. Inouye, and S. Kawata, Tip-enhanced coherent anti-stokes raman scattering for vibrational nanoimaging, Phys. Rev. Lett. 92(22), 220801 (2004).
10. Y. Fujita, P. Walke, S. D. Feyter, and H. Uji-i, Jpn. Tip-enhanced Raman scattering microscopy: Recent advance in tip production, Jpn. J. Appl. Phys. 55(8s1), 08NB03 (2016).
11. S. Berweger, J. M. Atkin, R. L. Olmon, and M. B. Raschke, Adiabatic Tip-plasmon focusing for nano-raman spectroscopy, J. Phys. Chem. Lett. 1(24), 3427–3432 (2010).
12. C. Ropers, C. C. Neacsu, T. Elsaesser, M. Albrecht, M. B. Raschke, and C. Lienau, Grating-coupling of surface plasmons onto metallic tips: a nanoconfined light source, Nano. Lett. 7(9), 2784–2788 (2007).
13. T. Umakoshi, M. Tanaka, Y. Saito, and P. Verma, White nanolight source for optical nanoimaging, Sci. Adv. 6(23), eaba4179 (2020).
14. X. Ma, Y. Zhu, N. Yu, S. Kim, Q. Liu, L. Apontti, D. Xu, R. Yan, and M. Liu, Toward high-contrast atomic force microscopy-tip-enhanced Raman spectroscopy imaging: nanoantenna-mediated remote-excitation on sharp-tip silver nanowire probes, Nano. Lett. 19(1), 100–107 (2019).
15. P. Walke, Y. Fujita, W. Peeters, S. Toyouchi, W. Frederickx, S. D. Feyter, and U. Hiroshi, Silver nanowires for highly reproducible cantilever based AFM-TERS microscopy: towards a universal ters probe, Nanoscale 10(16), 7556–7565 (2018).
16. M. Kauranen, and A. V. Zayats, Nonlinear plasmonics, Nat. Photon. 6(11), 737–748 (2012).
17. P. B. Johnson, and R. W. Christy, Optical constants of the noble metals, Phys. Rev. B 6, 4370–4379 (1972).
18. L. Novotny, and C. Hafner, Light propagation in a cylindrical waveguide with a complex, metallic, dielectric function, Phys. Rev. E 50(5), 4094-4106 (1994).
19. M. Esmann, S. F. Becker, B. B. da Cunha, J. H. Brauer, R. Vogelgesang, P. Groß, and C. Lienau, k-space imaging of the eigenmodes of sharp gold tapers for scanning near-field optical microscopy, Beilstein J. Nanotechnol. 4, 603-610 (2013).
20. F. Lu, W. Zhang, L. Huang, S. Liang, D. Mao, F. Gao, T. Mei, and J. Zhao, Mode evolution and nanofocusing of grating-coupled surface plasmon polaritons on metallic tip, Opto-Electron. Adv. 1(6), 18001001–18001007 (2018).
21. M. I. Stockman, Nanofocusing of optical energy in tapered plasmonic waveguides, Phys. Rev. Lett. 93(13), 137404 (2004).
22. S. Berweger, J. M. Atkin, R. L. Olmon, and M. B. Raschke, Light on the tip of a needle: plasmonic nanofocusing for spectroscopy on the nanoscale, J. Phys. Chem. Lett. 3(7), 945–952 (2012).
23. B. Ren, G. Picardi, B. Pettinger, Preparation of gold tips suitable for tip-enhanced Raman spectroscopy and light emission by electrochemical etching, Rev. Sci. Instrum. 75, 837-841 (2004).
24. S. Kim, N. Yu, X. Ma, Y. Zhu, Q. Liu, M. Liu, and R. Yan, High external-efficiency nanofocusing for lens-free near-field optical nanoscopy, Nat. Photon. 13(9), 636–643 (2019).